

# Melt-Intercalation Nanocomposites with Chlorinated Polymers

Younghoon Kim, James L. White

Institute of Polymer Engineering, The University of Akron, Akron, Ohio 44325

Received 4 October 2002; accepted 2 January 2003

**ABSTRACT:** Polyolefins and chlorine-containing polymers were investigated to produce polymer nanocomposites. Natural and organic-treated montmorillonite clays were melt compounded with the polymers. Organic-treated montmorillonite clay dispersed well in polychloroprene, chlorinated-polyethylene, polyvinyl chloride, chlorinated-polyvinyl chloride, and polyvinylidenechloride polymers, and formed nanocomposites. They were not well dispersed in polyolefins that contain no chlorine. X-ray diffraction and transmission electron microscopy techniques indicated the

separation of montmorillonite layers and indicated the formation of polymer nanocomposites in chlorine-containing polymers. Mechanical testing showed enhanced tensile strength and Young's modulus of chlorinated-polymers/clay compounds, but not polyolefins/clay compounds. © 2003 Wiley Periodicals, Inc. *J Appl Polym Sci* 90: 1581–1588, 2003

**Key words:** nanocomposites; clay; chlorinated polymers; compounding; *d* spacing

## INTRODUCTION

Polymer nanocomposites have become a new promising area in polymer research. Among the particles used to form nanocomposites are particular clays in which the intersilicate layers are swollen. The clays studied so far are mainly organically modified montmorillonites. *In situ* polymerization with monomers and melt intercalation with polymers are two major methods to make polymer nanocomposites.

Intracrystalline swelling of montmorillonite with water was probably known to the ancients. Since the discovery of intracrystalline swelling in montmorillonite by polar organic liquids in the 1930s,<sup>1,2</sup> there have been many studies of this phenomenon. Bradley<sup>3</sup> studied the interaction between montmorillonite and various organic liquids. Norrish<sup>4</sup> investigated the swelling of montmorillonite in salt solutions. The cation exchanging capability of montmorillonite organic amines and intercalation of organic molecules was explored.<sup>5</sup> It was found that some organic monomers are adsorbed by sodium montmorillonite.<sup>6</sup> The spontaneous polymerization of hydroxymethacrylate monomers in a montmorillonite–monomer mixture has been reported.<sup>7</sup>

In the 1980s, the Toyota Research Center refocused on the swelling behavior of montmorillonite by organic solvents.<sup>8</sup> The Toyota laboratory exchanged cat-

ions of montmorillonite (MMT) with several organic compounds and swelled the organic-treated MMT with the organization of polar hydrocarbon monomer,  $\epsilon$ -caprolactam. They succeeded in producing intercalated polyamide-6 nanocomposite by *in situ* polymerization.<sup>9–13</sup>

The orientation of MMT and nylon-6 crystallites<sup>14</sup> and mechanical properties<sup>15</sup> in nylon-6–clay nanocomposites were investigated. Polyamide-6–clay nanocomposites at low clay levels had unexpected higher tensile modulus and strength than pure polyamide-6. They licensed this invention to Ube Kosan, which commercialized Nylon Clay Hybrid (NCH) based upon polyamide-6.

Scientists around the world have subsequently investigated producing polymer nanocomposites from thermoplastics and succeeded with various polymers. These include polyamide-12 (PA12),<sup>16</sup> polycaprolactone (PCL),<sup>17</sup> polyethylene terephthalate (PET),<sup>18</sup> and polyvinyl chloride.<sup>19,20</sup> These polymers are generally polar. There have also been efforts at using compatibilizing agents with nonpolar polymers to produce nanocomposites.<sup>21–26</sup>

In this article, we seek to produce nanocomposites from polymers with different degrees of chlorination. Chlorination should increase polarity level. These are listed in Table I. In terms of increasing levels of chlorine level we consider polyolefins, polyethylene (PE) and polypropylene (PP), where the chlorine level is zero, polychloroprene (CR), chlorinated-polyethylene (C-PE), polyvinyl chloride (PVC), chlorinated-polyvinyl chloride (C-PVC), and polyvinylidenechloride

Correspondence to: James L. White.

TABLE I  
Characteristics of Polymer Materials

Materials	Chlorine content (wt %)	Commercial name	Dielectric constant <sup>c</sup>	Supplier
PE	None	2045 LLDPE	2.3	Dow Chemical
PP	None	8000 GK	2.25	Equistar Chemical
CR	40 <sup>a</sup>	Neoprene	4.9	DuPont Dow Elast.
C-PE	36 <sup>b</sup>	Tyryn	4.3–5.1	DuPont Dow Elast.
PVC	56.7 <sup>a</sup>	334FG	3.4	OxyVinyl
C-PVC	63.5 <sup>b</sup>	TempRite	3.1	Noveon
PVDC	> 71.5 <sup>a</sup>	Saran	4.67	Dow Chemical

<sup>a</sup> Calculation with molecular structure and atomic weight.

<sup>b</sup> Material data sheet.

<sup>c</sup> At 1 kHz, *Encyclopedia of Chemical Technology and Polymer Handbook*.

(PVDC). These were studied with organic-treated montmorillonite and natural sodium montmorillonite for comparison.

## EXPERIMENTAL

### Materials

Two nonpolar thermoplastics, PE and isotactic PP, were used. The PE and PVDC from Dow Chemical Co., CR and C-PE from DuPont Dow Elastomers, PVC from OxyVinyl Company, PP from Equistar Chemicals, C-PVC from Noveon, Inc., were kindly provided. The characteristics of these polymers and their suppliers are contained in Table I. We include dielectric constants to represent levels of polarity.

Southern Clay Co., supplied MMT clays (Cloisite™ 30B, and Na<sup>+</sup>). Cloisite™ 30B is an organic-treated MMT with a ternary ammonium salt. Cloisite™ Na<sup>+</sup> is a natural MMT.

In melt compounding of rigid PVC and C-PVC, a tin thermal stabilizer of Atofina Co. was premixed.

### Compounding

Compounding was carried out in a Brabender internal mixer at 180°C, 100 rpm with the various thermoplastics (PE, PP, CR, C-PE, PVC, C-PVC, PVDC). The polymers and clay (wt %) were premixed in beaker. CR, because of the double bond in its backbone, was mixed at 100°C.

### Characterization

A Bruker™ X-ray machine with  $\lambda$  (wavelength) = 1.5422 Å was used. Powder diffraction patterns were prepared.

Ultrathin sectioning ( $\leq 100$  nm) was performed using the Reichert Ultracut sectioning system. A transmission electron microscope (ZEOL ZEM-1200EXII) operated at 120 kV was used for taking images of the specimens.

Dog-bone-shaped specimens were prepared by compression molding for tensile testing in an Instron™ tensile machine. ASTM D638 method was used for rigid plastic materials and ASTM D412 for elastomeric materials. No mechanical testing was done for CR due to the shrinkage of molded specimens if they were not vulcanized. Vulcanization during molding introduces another variable, which we did not wish to treat at this time.

## RESULTS

### Clay

Cloisite™ Na<sup>+</sup> natural MMT was observed to have  $d$  spacing = 11.7 Å at  $2\theta = 7.55^\circ$  (Fig. 1). The organic-treated montmorillonite Cloisite™ 30B clay exhibited peak at  $2\theta = 4.78^\circ$ , which represents basal spacing ( $d$  spacing) = 18.5 Å.

### PE compounds

The X-ray diffraction (XRD) studies of these compounds showed no change in the diffraction pattern of

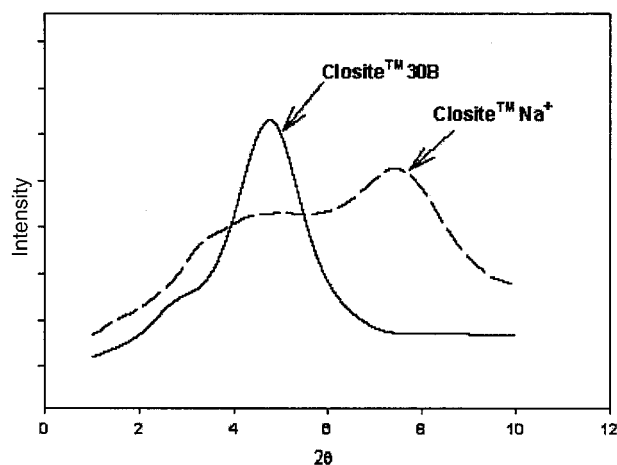


Figure 1 XRD of Cloisite™ 30B and Na<sup>+</sup> montmorillonite clays.

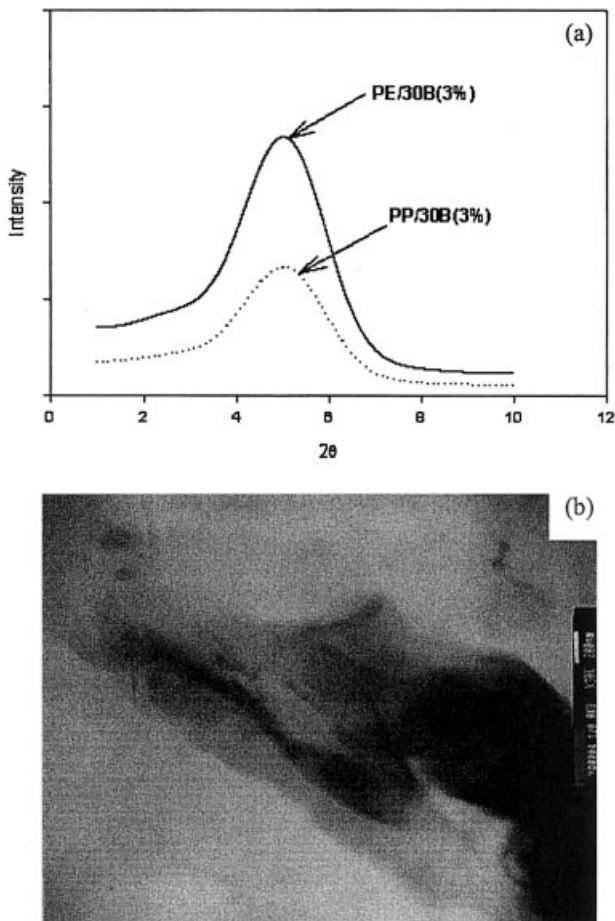


Figure 2 (a) XRD and (b) TEM of PE/30B and PP/30B compounds.

the natural MMT clay (Cloisite™ Na<sup>+</sup>) and organic-treated MMT (Cloisite™ 30B) clay in the PE polymer matrix [Fig. 2(a)]. The *d*-spacing peaks of both clays were not shifted to lower 2θ angles. PE crystallizes into the Bunn orthorhombic crystal structure and exhibits XRD peaks associated with its crystalline arrangement.

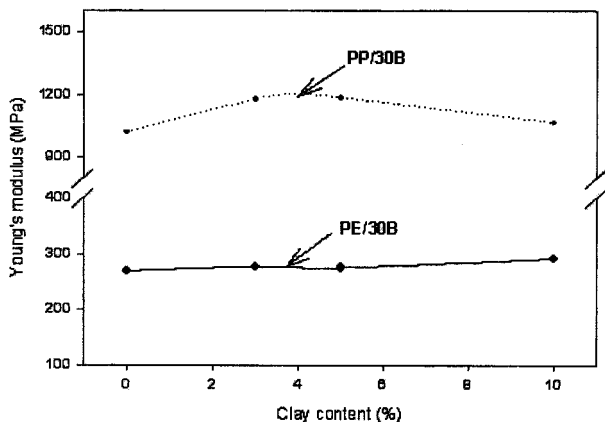


Figure 3 Young's modulus of PE/30B and PP/30B compounds.

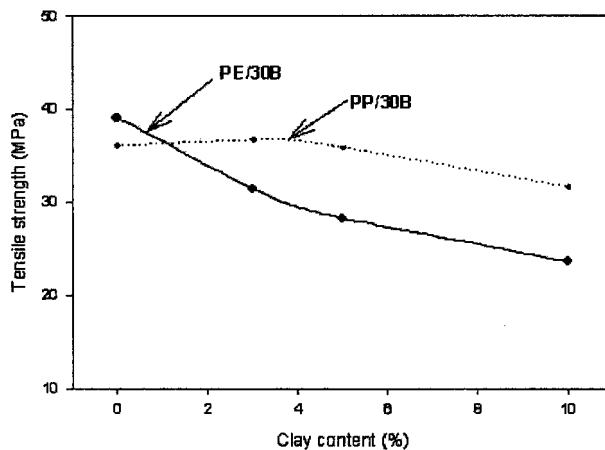


Figure 4 Tensile strength of PE/30B and PP/30B compounds.

The transmission electron microscopy (TEM) photomicrographs showed agglomerates of organic-treated MMT clay (Cloisite™ 30B) in the PE polymer matrix [Fig. 2(b)]. It suggests that the silicate layers were not separated by PE polymer chains.

The Young's modulus of PE/30B compounds was increased with clay content (Fig. 3). PE/30B(3%) and PE/30B(5%) had a 3 and 2% increase, respectively. PE/30B(10%) showed a 8% growth of modulus. The tensile strength of PE/30B compounds was reduced as clay content increased (Fig. 4). PE/30B(3%) had a 20% decreasing tensile strength. PE/30B(5%) and PE/30B(10%) exhibited a 28 and 40% decline correspondingly. The elongation at break of PE/30B compounds also showed a decrease (Fig. 5).

**PP compounds**

Isotactic PP crystallizes into the Natta and Corradini α monoclinic structure. The natural MMT clay (Cloisite™ Na<sup>+</sup>) and organic-treated MMT (Cloisite™ 30B) clay in the PP polymer matrix did not show separation of clay layers from XRD results ([Fig. 2(a)]. The 2θ angle of PP/30B and PP/Na<sup>+</sup> mixtures are close to the original 2θ angle of pure clays.

The TEM photomicrographs of the PP/30B compound also showed agglomerates of organic-treated MMT clay (Cloisite™ 30B) and suggested no separation of clay layers.

PP/30B compounds showed a higher modulus than pure PP (Fig. 3). PP/30B(3%) and PP/30B(5%) had a 15 and 16% increased Young's modulus. PP/30B(10%) had a 5% increased modulus. The PP/30B(3%) and PP/30B(5%) showed a 2% increased and 1% decreased tensile strength, respectively (Fig. 4). PP/30B(10%) had a 12% decrease in tensile strength. There were large reductions in elongation at break of PP/30B compounds compared to pure PP (Fig. 5).

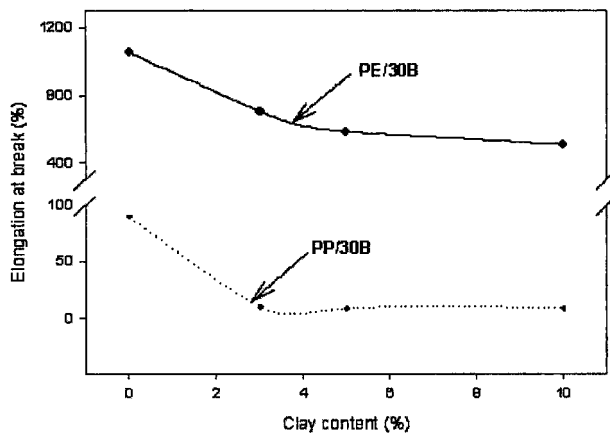


Figure 5 Elongation at break of PE/30B and PP/30B compounds.

**CR compounds**

There was no shift in the clay XRD peaks of natural MMT (Cloisite™ Na<sup>+</sup>) clay layers in the CR polymer.

Figure 6(a) shows the XRD test result of CR/30B compounds. The clay peaks of CR/30B(3%) and CR/30B(5%) were shifted to a lower angle at  $2\theta = 2.35$  and

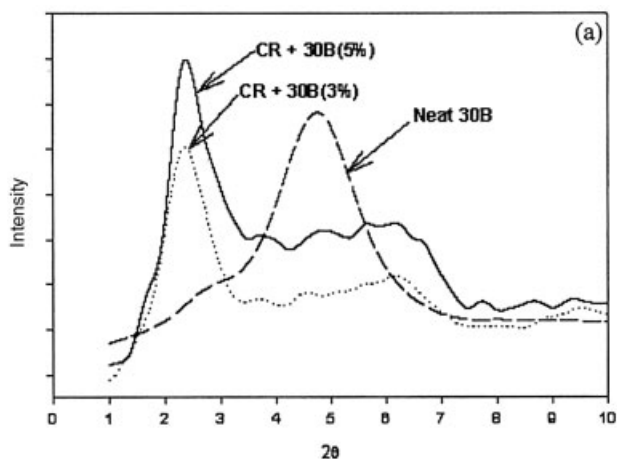


Figure 6 (a) XRD and (b) TEM of CR/30B compounds.

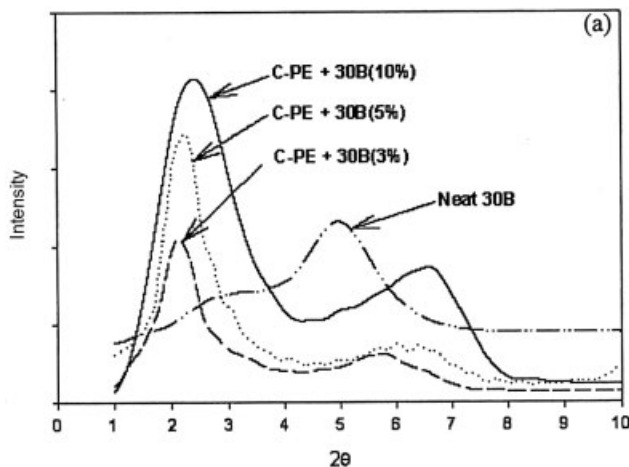


Figure 7 (a) XRD and (b) TEM of C-PE/30B compounds.

2.4°, which corresponds to 37.6 and 36.8 Å. These lower angle clay peaks represent expansion of basal spacing of clay layers in CR/30B compounds.

The TEM photomicrograph suggests clay separation of CR/30B compounds [Fig. 6(b)]. CR polymer chains intercalated clay particles. The penetration of CR polymer chains into clay layers can be surmised from the TEM result and XRD analysis.

**C-PE compounds**

The natural MMT (Cloisite™ Na<sup>+</sup>) clay layers did not show changes in *d* spacing in the C-PE compounds.

The XRD confirmed the separation of clay particles in C-PE/30B compounds [Fig. 7(a)]. The clay peak of C-PE/30B(3%) was shifted to a lower angle of  $2\theta = 2.1^\circ$ , which is equivalent for *d* spacing = 42.0 Å in comparison with the original *d* spacing (=18.5 Å) of Cloisite™ 30B clay. C-PE/30B(5%) and C-PE/30B(10%) also had their silicate layer peaks shifted to lower angles.

The TEM photomicrograph of C-PE/30B compound suggests C-PE polymer chains separated the clay layers of Cloisite™ 30B modified MMT clay [Fig. 7(b)].

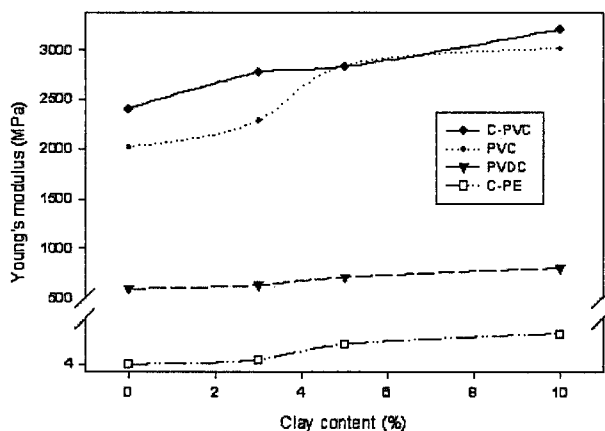


Figure 8 Young's modulus of chlorinated polymer/30B compounds.

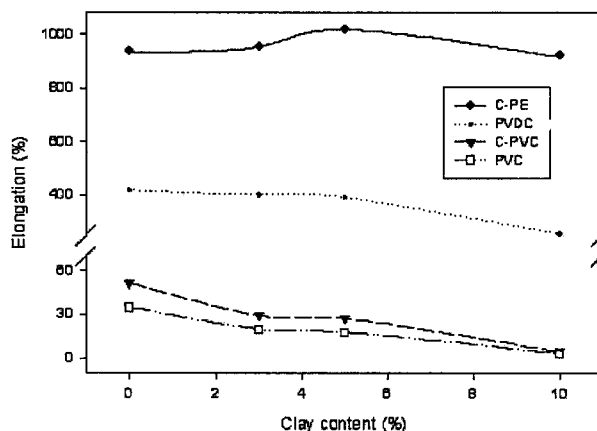


Figure 10 Elongation at break of chlorinated polymer/30B compounds.

Tensile tests were again used to determine mechanical behavior of C-PE/30B compounds at room temperature. The Young's modulus of C-PE/30B compounds increased with clay content (Fig. 8). C-PE/30B(3%) exhibited an 8% enhanced Young's modulus compared to pure C-PE. C-PE/30B(5%) and C-PE/30B(10%) showed 33 and 50% elevated modulus, respectively. Increasing clay content enhanced tensile strength of the C-PE/30B compound (Fig. 9). The tensile strength of C-PE/30B(3%) had a 5% increase over the pure C-PE. C-PE/30B(5%) and C-PE/30B(10%) also showed 31 and 21% growth in tensile strength. The elongation at break of C-PE/30B compounds was slightly decreased (Fig. 10).

PVC compounds

There was no change of the clay wide angle X-ray diffraction of the natural MMT clay (Cloisite™ Na<sup>+</sup>) in the PVC polymer matrix.

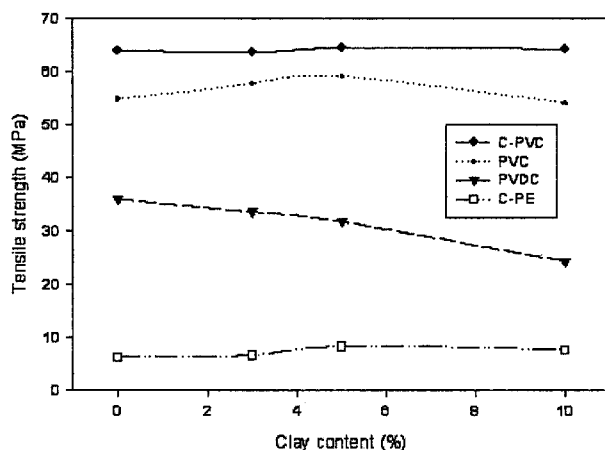


Figure 9 Tensile strength of chlorinated polymer/30B compounds.

The TEM image and XRD, however, indicate some breakup of the clay platelets of Cloisite™ 30B modified montmorillonite clay in the PVC polymer matrix.

The clay peak of the organically treated 30B of PVC/30B compound was shifted from  $2\theta = 4.78-2.56^\circ$ , which corresponds to  $d$  spacing = 34.5 Å [Fig. 11(a)]. PVC/30B(5%) and PVC/30B(10%) also have

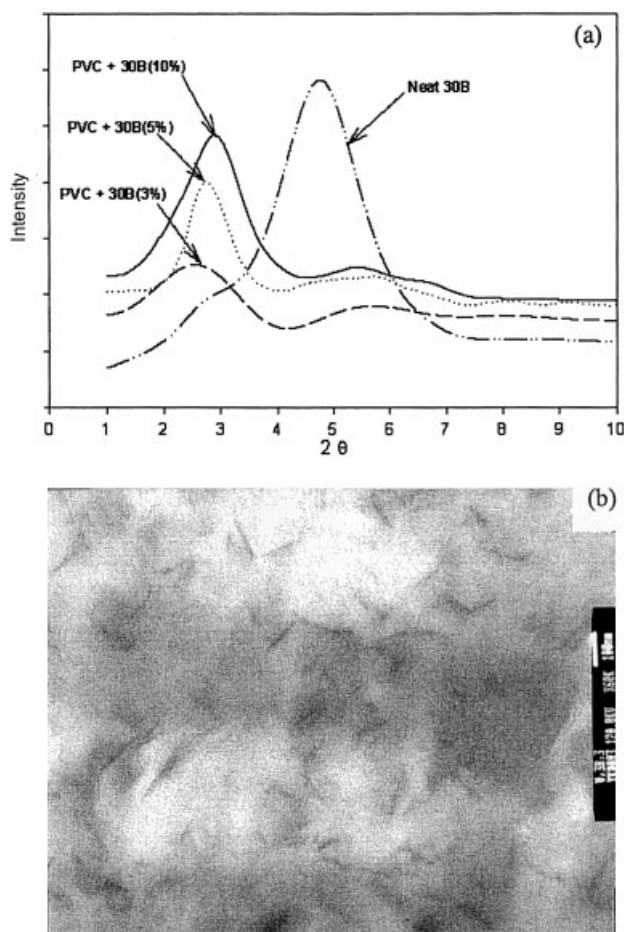
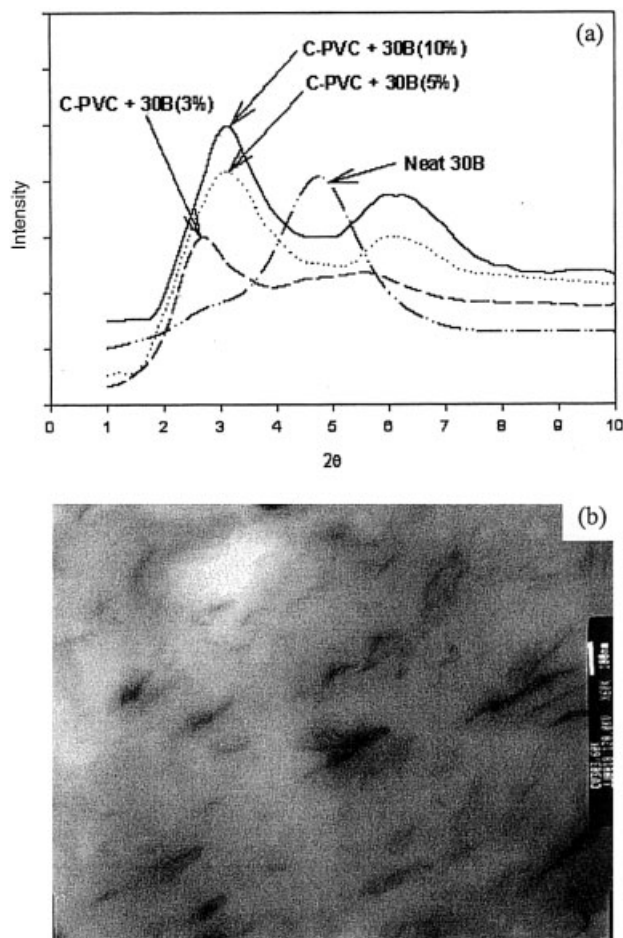


Figure 11 (a) XRD and (b) TEM of PVC/30B compounds.



**Figure 12** (a) X-ray diffraction and (b) TEM of C-PVC/30B compounds.

their clay peaks at lower angles. The PVC/30B(3%) compound showed the largest silicate separation.

The TEM photomicrograph of Figure 11(b) suggests clay particle breakup at the nanometer scale. The TEM image of PVC/30B(3%) shows separation of clay layers. The thickness of separated clay layers in PVC/30B(3%) is about 10–50 nm by the TEM image scale (= 100 nm).

The mechanical properties of PVC/30B compounds were evaluated in a uniaxial mechanical test. The Young's modulus of PVC/30B compounds was improved as clay content increased (Fig. 8). PVC/30B(3%) had a 13% improved Young's modulus than pure PVC. PVC/30B(5%) and PVC/30B(10%) had a 24 and 50% higher modulus than pure PVC, respectively. The tensile strength of PVC/30B(3%) and PVC/30(5%) was improved (Fig. 9). PVC/30B(3%) had 5% and PVC/30B(5%) had 8% enhanced tensile strength. PVC/30B(10%) showed 8% less tensile strength than pure PVC. The elongation at break of PVC/30B compounds decreased with clay content (Fig. 10).

### C-PVC compounds

No change in X-ray data was observed in the C-PVC polymer and natural MMT (Cloisite™ Na<sup>+</sup>) clay compound.

For the organic-modified clay, Figure 12(a) shows the XRD result for the C-PVC/30B compounds. The clay X-ray peaks of C-PVC/30B(3%) have shifted to  $2\theta = 2.7^\circ$ ,  $d$  spacing = 32.7 Å. The original  $d$  spacing of Cloisite™ 30B clay is 18.5 Å. The clay peaks of C-PVC/30B(5%) and C-PVC/30B(10%) were also shifted to lower angles.

The TEM image of C-PVC/30B compound shows clay dispersion [Fig. 12(b)]. It suggests that the C-PVC polymer takes apart clay layers. The individual thickness of each clay layer can be evaluated to be around 10 nm by the TEM image scale.

The Young's modulus of C-PVC/30B compounds was enhanced with increasing clay content (Fig. 8). C-PVC/30B(3%) showed 15% growth of Young's modulus than pure C-PVC. C-PVC/30B(5%) and C-PVC/30B(10%) had a 18 and 33% raised modulus correspondingly. There was no noticeable relationship between tensile strength and clay content of C-PVC/30B compounds (Fig. 9). The elongation at break of C-PVC/30B compounds was decreased (Fig. 10).

### PVDC compounds

There was no separation of the natural MMT (Cloisite™ Na<sup>+</sup>) clay particles in PVDC compounds. The characteristic of the PVDC/Cloisite™ 30B compounds was determined by XRD and TEM test results.

PVDC/30B(3%) exhibited a clay peak at lower angle  $2\theta = 2.6^\circ$ ,  $d$  spacing = 34 Å [Fig. 13(a)]. The original Cloisite™ 30B clay had a  $d$  spacing = 18.5 Å. The  $d$  spacing of PVDC/30B(5%) and PVDC/30B(10%) was increased as well.

The clay platelets were fairly well dispersed in PVDC polymer matrix [Fig. 13(b)]. There were no clay agglomerates in the TEM image of PVDC/30B compounds. The various thicknesses of individual clay layers could be estimated as less than 50 nm by the TEM image scale.

PVDC/30B compounds had an enhanced Young's modulus (Fig. 8). PVDC/30B(3%) showed a 6% raised Young's modulus than pure PVDC. PVDC/30B(5%) and PVDC/30B(10%) also had a 20 and 36% improved modulus. The tensile strength of PVDC/30B compounds decreased (Fig. 9). PVDC/30B(3%) exhibited a 7% tensile strength drop compared to pure PVDC. PVDC/30B(5%) and PVDC/30B(10%) showed a 12 and 32% decreased tensile strength. The elongation at break of PVDC/30B compounds decreased with clay content (Fig. 10).

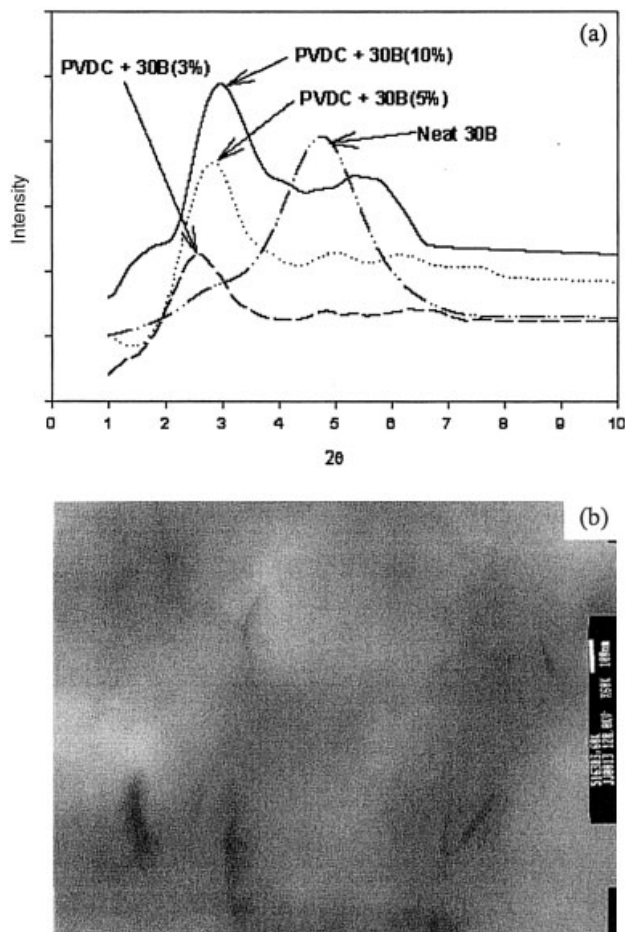


Figure 13 (a) XRD and (b) TEM of PVDC/30B compounds.

## DISCUSSION

### Nanocomposite structure and mechanism

The MMT clay is a phyllosilicate mineral. Cations such as  $\text{Na}^+$ ,  $\text{K}^+$ , and  $\text{Ca}^{2+}$ , compensate the negative charge that exists in each layer due to altered replacement in the crystal lattice of the layer. Water and other polar molecules can penetrate between the layers and swell MMT clay. Cloisite™ 30B is an organic-treated MMT clay with a ternary ammonium salt. It has an organic functional group between clay layers. It is more organophilic (i.e., hydrophobic) than natural montmorillonite clay (Cloisite™  $\text{Na}^+$ ). Our experience indicates polymer chains penetrate between organic-treated clay layers more easily.

PE ( $-\text{[CH}_2-\text{CH}_2\text{]}_n-$ ) and PP ( $-\text{[CH}_2-\text{CHCH}_3\text{]}_n-$ ) are important polyolefins. They are non-polar polymers and the clay environments are hostile to them. This is true of both the natural and organic-treated clays.

The chlorinated polymers are also incompatible with the natural clays. This is not the case with the organic-treated clays. The polarity of chlorinated polymer chains and organophilicity of the organic-treated

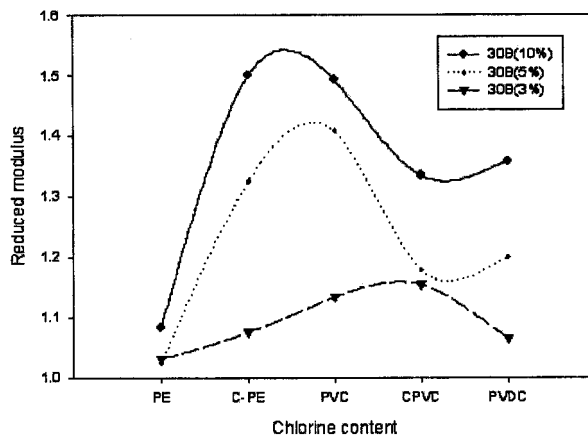


Figure 14 Reduced Young's modulus vs chlorine content.

MMT clay allow the formation of chlorinated polymer nanocomposites.

The results cited here are in agreement with earlier investigations with PVC<sup>19,20</sup> and extend the observations to a wide range of chlorinated polymers.

### Mechanical properties

The Young's modulus of all chlorinated polymers with Cloisite™ 30B compounds increased with clay content but not polyolefins (Fig. 14). The tensile strength notably of the C-PE is increased (Fig. 15).

These changes in level of mechanical properties are similar to those reported by other investigations. They found an increase in Young's modulus and tensile strength for PVC.

There seems a maximum effect in chlorine content. This is at the C-PE and PVC levels of chlorine content. The enhancement of properties with C-PVC and especially PVDC seems reduced.

## CONCLUSION

The Cloisite™ 30B modified MMT clay was well dispersed in CR, C-PE, PVC, C-PVC, and PVDC polymer

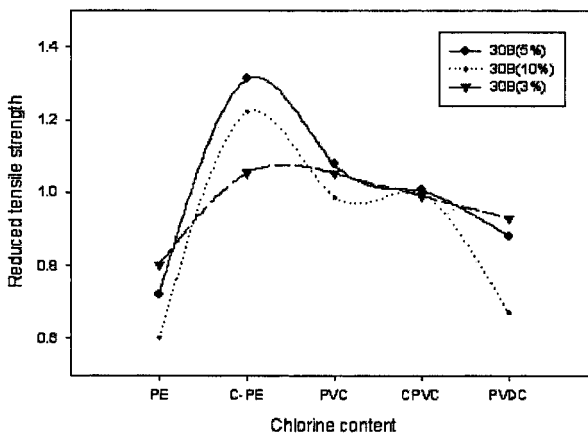


Figure 15 Reduced tensile strength vs chlorine content.

matrices. There was no intercalation of clay layers in PE and PP. The polarity of the chlorinated polymers and organophilic property of modified MMT clays could be the reason of the formation of nanocomposites. XRD and TEM characterizations proved intercalation of clay platelets. Mechanical properties of the polymer nanocomposites were enhanced in comparison with that of pristine polymers.

This research was supported in part by the Edison Polymer Innovation Corporation.

## References

1. Hofmann, U.; Endell, K.; Wilm, D. *Z Kristallogr, Mineralog Petrogr Ab A* 1933,86, 340.
2. Hofmann, U.; Endell, K.; Wilm, D. *Angew Chem* 1934, 47, 539.
3. Bradley, W. F. *J Amer Chem Soc* 1945, 67, 975.
4. Norrish, K. *Disc Faraday Soc* 1954, 18, 120.
5. Weiss, A. *Angew Chem Int Ed* 1963, 2(3), 134.
6. Blumstein, A. *J Polym Sci A* 1965, 3, 2653.
7. Solomon, D. H.; Loft, B. C. *J Appl Polym Sci* 1968, 12,1253.
8. Fukushima, Y.; Inagaki, S. *J Incl Pheonom* 987, 5, 473.
9. Fukushima, Y.; Okada, A.; Kawasumi, M.; Kurauchi, T.; Kamigaito, O. *Clay Materials* 1988,23, 27.
10. Usuki, A.; Kojima, Y.; Kawasumi, M.; Okada, A.; Fukushima, Y.; Kurauchi, T.; Kamigaito, O. *J Mater Res* 1993, 8(5), 1179.
11. Kojima, Y.; Usuki, A.; Kawasumi, M.; Okada, A.; Kurauchi, T.; Kamigaito, O. *J Polym Sci, Part A: Polym Chem* 1993, 31, 983.
12. Usuki, A.; Kawasumi, M.; Kojima, Y.; Okada, A.; Kurauchi, T.; Kamigaito, O. *J Mater Res* 1993, 8(5), 1174.
13. Kojima, Y.; Usuki, A.; Kawasumi, M.; Okada, A.; Kurauchi, T.; Kamigaito, O. *J Polym Sci, A: Polym Chem* 1993, 31, 1755.
14. Kojima, Y.; Usuki, A.; Kawasumi, M.; Okada, A.; Kurauchi, T.; Kamigaito, O.; Kaji, K. *J Polym Sci, B: Polym Phys* 1994, 32, 625.
15. Kojima, Y.; Usuki, A.; Kawasumi, M.; Okada, A.; Fukushima, Y.; Kurauchi, T.; Kamigaito, O. *J Mater Res* 1993, 8, 1185.
16. Hoffmann, B.; Kressler, J.; Stoppelmann, G.; Friedrich, Chr.; Kim, G.-M. *Colloid Polym Sci* 2000, 278, 629.
17. Messersmith, P. B.; Giannelis, E. P. *J Polym Sci, A: Polym Chem* 1995, 33, 1047.
18. Ke, Y.; Long, C.; Qi, Z. *J Appl Polym Sci* 1999, 71, 1139.
19. Wang, D.; Parlow, D.; Yao, Q.; Wilkie, C. A. *J Vinyl Additive Tech* 2001, 7, 203.
20. Hinojosa-Falcon, L. A.; Goettler, L. A. *SPE ANTEC Tech Paper* 2002, 2, 1509.
21. Kawasumi, M.; Hasegawa, N.; Kato, M.; Usuki, A.; Okada, A. *Macromolecules* 1997,30, 6333.
22. Usuki, A.; Kato, M.; Okada, A. T. Kurauchi, J. *J Appl Polym Sci* 1997, 63, 137.
23. Kato, M.; Usuki, A.; Okada, A. *J Appl Polym Sci* 1997, 66, 1781.
24. Hasegawa, N.; Kawasumi, M.; Kato, M.; Usuki, A.; Okada, A. *J Appl Polym Sci* 1998,67, 87.
25. Hasegawa, N.; Okamoto, H.; Kato, M.; Usuki, A. *J Appl Polym Sci* 2000, 78, 1918.
26. Fischer, H. F.; Gielgens, L. H.; Koster, T. P. M. *Acta Polym* 1999, 50, 122.